Compression and localization of an atomic cloud in a time dependent optical lattice

Will Williams
wdwilliams@wisc.edu

M. Saffman
Department of Physics, 1150 University Avenue, University of Wisconsin-Madison, Madison, WI, 53706

Abstract: We analyze a method to compress a cloud of cold atoms in a far off resonance optical lattice by dynamically changing the lattice parameters while cooling the atoms with optical molasses. Particle motion in the time dependent lattice is studied numerically using a three dimensional semiclassical model. We show that smoothly varying the lattice spacing from a large to a small value results in compression of more than 75% of the atoms initially in a Gaussian distributed cloud with standard deviation of 50 μm into a single site of a two-dimensional lattice. The lattice site has an area of $A = 0.76\ \lambda^2$ with λ the wavelength of the trapping beam. We demonstrate that an increase in the optical depth by a factor of at least 175 is possible.

OCIS codes: 020.7010,140.7010,140.3320,230.6120

References and links

[1] S. Chu, J. E. Bjorkholm, A. Ashkin, and A. Cable, "Experimental Observation of Optically Trapped Atoms," Phys. Rev. Lett. **57**, 314 (1986).

[2] J. D. Miller, R. A. Cline, and D. J. Heinzen, "Far-Off-Resonance Optical Trapping of Atoms," Phys. Rev. A **47**, R4567 (1993).

[3] M. D. Barrett, J. A. Sauer, and M. S. Chapman, "All-Optical Formation of an Atomic Bose-Einstein Condensate," Phys. Rev. Lett. **87**, 010404 (2001).

[4] T. Kinoshita, T. Wenger, and D. S. Weiss, "All-optical Bose-Einstein condensation using a compressible crossed dipole trap," Phys. Rev. A **71**, R011602 (2005).

[5] T. P. Meyrath, F. Schreck, J. L. Hanssen, C. S. Chuu, and M. G. Raizen, "A high frequency optical trap for atoms using Hermite-Gaussian beams," Opt. Express **13**, 2843 (2005).

[6] S. Bergamini, B. Darquié, A. Browaeys, and P. Grangier, "Single atoms in optical traps," J. Phys. IV **116**, 205 (2004).

[7] D. Schrader, I. Dotsenko, M. Khudaverdyan, Y. Miroshnychenko, A. Rauschenbeutel, and D. Meschede, "Neutral Atom Quantum Register," Phys. Rev. Lett. **93**, 150501 (2004).

[8] D. D. Yavuz, P. B. Kulatunga, E. Urban, T. A. Johnson, N. Proite, T. Henage, T. G. Walker, and M. Saffman, "Fast Ground State Manipulation of Neutral Atoms in Microscopic Optical Traps," Phys. Rev. Lett. **96**, 063001 (2006).

[9] J. Sebby-Strabley, R. T. R. Newell, J. O. Day, E. Brekke, and T. G. Walker, "High-density mesoscopic atom clouds in a holographic atom trap," Phys. Rev. A **71**, R021401 (2005).

[10] M. Saffman and T. G. Walker, "Entangling single and N atom qubits for fast quantum state detection and transmission," Phys. Rev. A **72**, 042302 (2005).

[11] M. G. Raizen, A. M. Dudarev, Q. Niu, and N. J. Fisch, "Compression of Atomic Phase Space Using an Asymmetric One-Way Barrier," Phys. Rev. Lett. **94**, 053003 (2005).

[12] M. Vengalattore, W. Rooijakkers, R. Conroy, and M. Prentiss, "Suppression of photon rescattering due to spatial anisotropy in a cold atomic gas," Phys. Rev. A **67**, 063412 (2003).

[13] S. L. Winoto, M. T. DePue, N. E. Bramall, and D. S. Weiss, "Laser cooling at high density in deep far-detuned optical lattices," Phys. Rev. A **59**, R19 (1999).

[14] S. Wolf, S. J. Oliver, and D. S. Weiss, "Suppression of Recoil Heating by an Optical Lattice," Phys. Rev. Lett. **85**, 4249 (2000).

[15] P. Rudy, R. Ejnisman, A. Rahman, S. Lee, and N. P. Bigelow, "An all optical dynamical dark trap for neutral atoms," Opt. Express **8**, 162 (2001).

[16] N. Friedman, L. Khaykovich, R. Ozeri, and N. Davidson, "Compression of cold atoms to very high densities in a rotating-beam blue-detuned optical trap," Phys. Rev. A **61**, R031403 (2000).

[17] J. J. McClelland, "Atom-Optical Properties Of A Standing-Wave Light-Field," J. Opt. Soc. Am. B **12**, 1761 (1995).

[18] W. Wohlleben, F. Chevy, K. Madison, and J. Dalibard, "An Atom Faucet," Eur. Phys. J. D **15**, 237 (2001).

[19] W. Ketterle, K. B. Davis, M. A. Joffe, A. Martin, and D. E. Pritchard, "High-Densities of Cold Atoms in a Dark Spontaneous-Force Optical Trap," Phys. Rev. Lett. **70**, 2253 (1993).

[20] V. Elman and A. Hemmerich, "Near-resonant dark optical lattice with increased occupation," Phys. Rev. A **72**(4), 043410 (2005).

[21] M. Vengalattore, R. S. Conroy, and M. G. Prentiss, "Enhancement of Phase Space Density by Increasing Trap Anisotropy in a Magneto-Optical Trap with a Large Number of Atoms," Phys. Rev. Lett. **92**, 183001 (2004).

[22] L.-M. Duan, J. I. Cirac, P. Zoller, and E. S. Polzik, "Quantum Communication between Atomic Ensembles Using Coherent Light," Phys. Rev. Lett. **85**, 5643 (2000).

[23] A. Haase, D. Cassettari, B. Hessmo, and J. Schmiedmayer, "Trapping neutral atoms with a wire," Phys. Rev. A **64**, 043405 (2001).

1. Introduction

During the last few decades there has been intense development of methods to cool and localize atomic samples with optical fields. Conservative trapping potentials can be created using far off resonance light beams that are focused to a small spot(1; 2). These far off resonance traps have become widely used as a starting point for achieving Bose Einstein condensation(3; 4; 5), as well as for experiments with single atoms(6; 7; 8). There is currently much interest in finding ways to load a large number of atoms at high densities into optical traps(9). This is important for creating large condensates, as well as highly localized atomic ensembles for quantum logic and communications(10). The phase space density of atomic clouds can be increased using laser or evaporative cooling as well as by novel approaches such as asymmetrical optical barriers(11). Heating due to photon rescattering limits the phase space density that can be reached by optical cooling although spatially anisotropic samples(12) as well as optimized cooling techniques in optical lattices(13; 14) have led to improved performance. Dynamically changing the optical potential in conjunction with optical cooling can also increase phase space density. Compression of an atomic cloud was also achieved in a trap created by rapidly rotating a single blue detuned beam(15; 16).

In this paper we present a method for compressing atoms in a MOT into a single well of a periodic optical lattice. We use numerical simulations to study the performance of a novel protocol for transferring a three-dimensional distribution of atoms into a single well of a planar lattice. The anisotropic well is elongated perpendicular to the plane of the lattice which minimizes heating and repulsion due to photon rescattering(12) and is well suited for applications that require mode matching between a Gaussian laser beam and a pencil shaped atomic ensemble(10). The technique can also be extended to a three dimensional lattice to create a spherically shaped localized cloud of atoms.

The proposed method is to dynamically change the angle between the lattice forming beams to confine the atoms in a single lattice site that is initially large, and is made smaller without the atoms escaping. This can be done conveniently using a one-dimensional spatial light modulator (SLM) with a linear array of N pixels as shown in Fig 1. Atoms of temperature T are localized within a distance $\delta r \sim w\sqrt{k_B T/U}$ from the origin in a well of depth U that is created by a focused laser beam with Gaussian waist w. The atoms have a vibrational oscillation frequency of $\nu = (2/w)\sqrt{U/m}$, where m is the mass of an atom. Provided the well is made smaller on a time scale that is long compared to the oscillation frequency, the atoms will tend to be trapped in the center of the well and get compressed. Under this adiabatic condition, optical molasses is not necessary to spatially compress the atoms but there will be no increase in phase space density. By combining the dynamic lattice reshaping with optical cooling the atoms can be compressed to higher phase space density.

The compression of the atomic cloud, which is described in detail in Sec. 2, is accomplished by using the SLM to change the angle between the lattice beams in a specified sequence. Section 3 presents results of numerical simulations that validate the proposal. Finally, Sec. 4 discusses applications and limitations of the technique as well as some alternative compression geometries.

2. Theory

We describe a technique to compress atoms in a single site of a two-dimensional lattice by dynamically changing the angles between the lattice beams. The conservative optical potential for a two-level atom including the effects of saturation is(17)

$$U(\mathbf{r}) = \frac{\hbar\Delta}{2}\ln\left[1+\frac{I(\mathbf{r})}{I_s}\frac{1}{(1+4\Delta^2/\gamma^2)}\right], \tag{1}$$

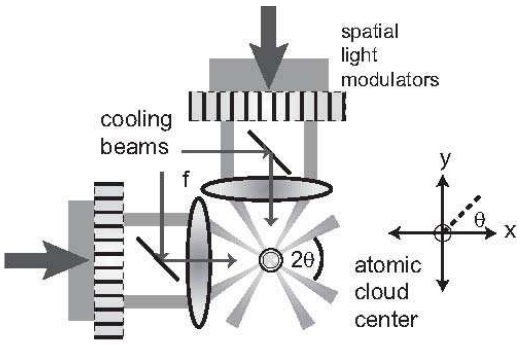

Fig. 1. Schematic of proposed setup. The setup consists of 2 SLMs which compress the atom cloud by dynamically controlling the amplitude of the laser beams. Additional cooling beams provide optical molasses during the compression.

where $I(\mathbf{r})$ is the optical intensity distribution, I_s is the saturation intensity, γ is the natural linewidth, $\Delta = \omega - \omega_a$ is the detuning from resonance, ω is the optical frequency, and ω_a is the atomic transition frequency.

Consider two equal intensity plane traveling waves with wavevectors $\mathbf{k}_j = k(\cos\theta_j\hat{x} + \sin\theta_j\hat{y})$ where k is the wavenumber and θ_j is the angle each beam makes with the $x-$axis. When θ_1=-θ_2=θ the angle between the beams is 2θ and the intensity is

$$I(x,y) = 4I_0\cos^2[k\sin(\theta)y] \tag{2}$$

where I_0 is the intensity of each wave. The periodicity of the intensity is thus $\Lambda(\theta) = \frac{\lambda}{2\sin(\theta)}$ where λ is the wavelength of the light. To achieve compression in one dimension θ is increased from 0 to $\pi/2$ radians. Doing so decreases the periodicity from infinity (a plane wave with uniform intensity) to $\frac{\lambda}{2}$, the periodicity of a single standing wave. To accomplish two dimensional compression another set of traveling waves are added with their bisector orthogonal to the bisector of the first pair as in the configuration shown in Fig. 1. By arranging for the second pair of waves to be polarized orthogonally to the first pair we obtain[1]

$$I(x,y) = 4I_0\left\{\cos^2[k\sin(\theta)x] + \cos^2[k\sin(\theta)y]\right\}. \tag{3}$$

This intensity produces a two dimensional lattice pattern with periodicity of Λ in both the x and y directions. Each site of the lattice has an area of $A(\theta) = \frac{\lambda^2}{4\sin^2(\theta)}$. As θ increases from 0, the area of each well decreases as shown in Fig. 2. If the initial value of θ is small enough the central well will be large enough to contain essentially all of the atoms. Any atoms that start in the central well will stay there during the compression of the wells as long as they are not hot enough to travel over the intensity barrier into the next well. If some of the atoms escape the central well, the method can be repeated to obtain better compression. A similar protocol is also possible using standing waves as will be discussed in Section 4.

The compression protocol thus relies on the following sequence. We start with a cloud of cold atoms and superimpose a two-dimensional lattice of optical trapping beams created by

[1] Superposition of the orthogonally polarized pairs of beams creates a field that has a spatially varying polarization state. In a real multilevel atom the optically induced potential depends on the polarization when there is a nonzero vector or tensor polarizability. We assume in this paper that polarization effects are negligible so that the potential is accurately described using the intensity of Eq. (3). This is true for alkali atom ground states provided the wavelength is sufficiently far detuned from the strong D lines.

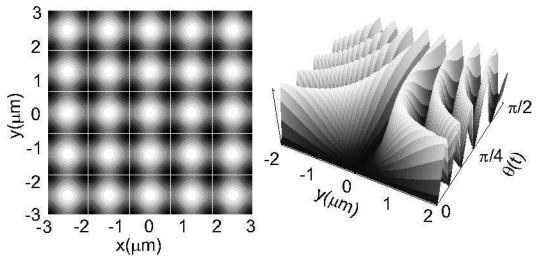

Fig. 2. Left: Contour Plot of the interference pattern created by four traveling waves, as described in the text, with $\theta = \pi/8$. Regions of higher intensity are shown in white. Thin white lines have been drawn between each row and column. Right: The intensity along the $y-$axis as a function of θ. When $\theta = 0$, there is a plane wave with equal intensity over all space. As θ increases, a two dimensional structure forms and the well area decreases. If the atoms are cool enough that they cannot travel over the intensity barrier, they are forced to compress as θ increases. Regions of higher intensity are shown in black here.

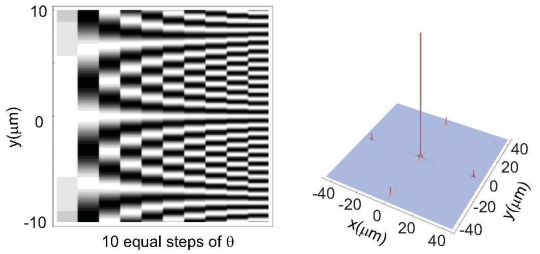

Fig. 3. (Color Online) Left: Contour plot of the intensity of the trap along the $y-$axis as θ changes by equal increments. Right: Number of atoms in the lattice at the end of a compression sequence with θ changing by 0.7 deg. at each step. If some of the atoms have a local minimum that is not the central well, they end up far from the central well, as shown by the secondary peaks.

two pairs of crossing beams propagating along $\hat{x}$ and $\hat{y}$ as shown in Fig. 1. The initial value of $\theta = \theta_{\min}$ is chosen small enough such that almost all the atoms are confined in the central lattice well. We then increase θ by a small step which spatially compresses the atoms but also heats them since the well area decreases. The increase in temperature is removed by applying optical molasses for a short cooling time T_c, after which the lattice beam angles are again changed. This sequence is repeated until the atoms have been compressed into a lattice site with small area created by the maximum crossing angle $\theta = \theta_{\max}$.

In a real experiment with a SLM there is a finite resolution with which the angle θ can be set. If θ is abruptly changed by too large an amount atoms may get trapped in a local minimum of the optical potential, and not be swept towards the center of the lattice as illustrated in Fig. 3. In addition if the initial value of θ is not small enough some of the atoms will not start in the central well and will not end up at the origin. To avoid these problems a large number of SLM pixels are needed so that the steps in θ are small (alternatively an analog scanning device such as an acousto-optic beam deflector or scanning mirror could be used). It is convenient if the amount of heating incurred at each step is approximately constant, since T_c can then be held constant. This will be the case if the fractional change in the area of each lattice site is held

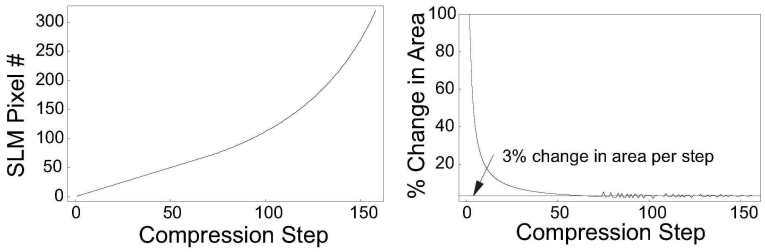

Fig. 4. Left: The number of the SLM pixel turned on at each step in the compression sequence. This represents the best possible fit allowed by the SLM for a 3% change in well area at each step. Right: Percent change in well area for the compression scheme as a function of compression step.

constant. In an experiment with a finite number of SLM pixels this requirement cannot be met exactly. For the simulations shown below we assumed the SLM's shown in Fig. 1 each had 640 pixels and that the range in θ was from $\theta_{\min} = 0.063$ to $\theta_{\max} = 35$ deg. The pixels used at each compression step were chosen to approximate as well as possible a 3% change in well area between steps, as shown in Fig. 4.

3. Numerical Results

Atomic compression was simulated numerically using Newtonian dynamics. The equation of motion $m\ddot{\mathbf{r}} = -\nabla U$ was used to update the velocity and position of each atom during the compression protocol. Interatomic collisions were not accounted for. The atomic parameters were chosen to correspond to the D2 transition of Cs ($6^2S_{1/2} - 6^2P_{3/2}$) at $\lambda = 852$ nm and with decay rate $\gamma = 2\pi \times 5.22$ MHz. The laser beams used to create the lattice potential were assumed transmitted through a SLM with rectangular pixels and then focused into the region containing the atomic sample as shown in Fig. 1. The SLM is assumed illuminated with an elliptically shaped Gaussian beam that is thinner than the height of each pixel but covers all of the SLM pixels in the $x-y$ plane. The lenses between the SLM and the atom trapping region provide a Fourier transform of the field distribution so that switching a single SLM pixel into the transmitting state results in a beam in the trapping region with a Gaussian envelope along z (perpendicular to the plane of the lattice), and a Sinc squared envelope in the plane. Provided that the width of the Sinc function is at least a few times larger than the size of the lattice site created at $\theta_{\min}$ the numerical results do not depend on the exact form of the transverse field distribution.

Comparing the difference between the intensity pattern created by a plane wave and a plane wave enveloped by a sinc squared function with FWHM $= 200$ μm, the only noteworthy difference is on the first step. For the first step, the atoms are not confined near the bottom of the well and the FWHM of the sinc squared is smaller than the FWHM of the central well created by plane waves by about 48%. This results in a different number of atoms lost on the first step. After step 1, the percent difference of the FWHM's drops rapidly and is below 1% by step 5. Since the atoms are confined near the bottom of the well after step 1, the small difference between the two potentials is negligible. We have therefore used interfering plane waves in the $x-y$ plane for the numerical work, and assumed the focused beams were circular with waists of $w_z = w_y = 100$ μm (for e.g. a beam propagating along $\hat{x}$) in calculations of optical power requirements.

The beam detuning was $\Delta = 2\pi \times 5$ GHz and the peak intensity was 2×10^6 W/m^2 which results in a well depth of $U_0/k_B = 6$ mK for the above parameters. This choice of detuning and

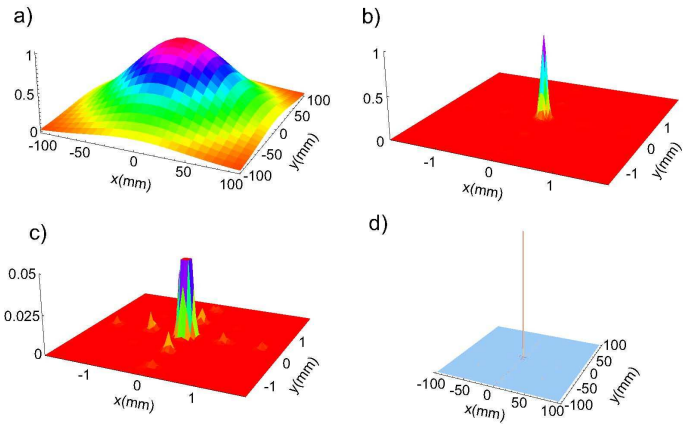

Fig. 5. (Color Online) The initial Gaussian distribution a), the final number density over 25 lattice sites b), the final number density over 25 lattice sites plotted to a maximum of 5% to show the atoms that have escaped into adjacent wells c), and a histogram with bins defined by the lattice area $A(\theta_{\max})$ to display the final compression results d).

intensity gives a scattering rate of 7.8×10^5 photons/sec and requires a total power of 5W for each pair of beams. This high power is a result of illuminating the entire SLM with a cylindrical beam whose parameters fit the width of the SLM but only opening two pixels at a time. Note that the effective well depth is only 3 mK since for traveling waves the wells are connected at 50% of the maximum intensity. For all simulations, discrete steps were used to compress the atoms, as discussed in Sec. 2.

Optical cooling is necessary since the atoms heat as they are being compressed. Cooling by three dimensional molasses was simulated by testing the probability that a photon is scattered at every time step using an approximation to the three dimensional distribution of the optical field as described in (18). If the atom scattered a photon, the atom's momentum was changed by $\hbar$k along the appropriate cooling beam for absorption and then in a random direction in three dimensions for emission. The dipole emission pattern of a real atom was approximated by a spherically uniform emission probability. The intensity of each cooling beam was set to 1.09 W/m^2, or $I/I_s = .1$ where I_s is the saturation intensity, and the detuning was set to $\Delta = -\gamma/2$. To avoid the effects of differential ground and excited state AC Stark shifts due to the lattice beams, the cooling and lattice beams were flashed on and off out of phase with each other at a rate of 4 MHz. The rate was sufficiently large compared to the highest vibrational frequency encountered to avoid loss of atoms during the periods when the lattice beams were off. The temperature of the atoms was monitored and when either the cooling time exceeded 3 ms or all three Cartesian components of the temperature were below 180 μK, the next step in compression was taken. The Doppler temperature for 6 cooling beams each with $I/I_s = .1$ is about 160 μK in the x,y, and z directions.

The initial atom distribution was a Gaussian with standard deviations of $\sigma_x = \sigma_y = \sigma_z = 50$ μm. The initial temperature was set to $T_a = 140$ μK in x,y and z. The cloud was then placed in the potential defined by the first step in the lattice compression. The simulation involves 158 steps and θ was allowed to vary between 0.063 and 35 deg. (a maximum of 70 deg. between two beams) according to the allowed values of θ produced by the SLM. We chose $\theta_{\max} = 35$ deg. to correspond to an experiment where there may only be 70 deg. of access on each side of the trapping region. This will produce a minimum lattice site area of $A(\theta_{\max}) \simeq 0.55$ μm^2.

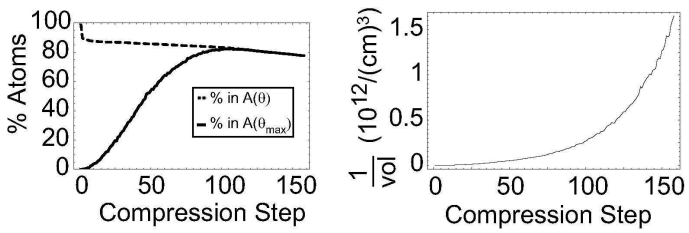

Fig. 6. Left: Percent of atoms captured within the minimum well area $A(\theta_{\max})$ per step of compression (solid line) and percentage of atoms captured in the central well(dashed line). Right: Plot of one over the effective volume for one atom per step of compression.

The results of a simulation run with 5000 atoms are shown in Fig. 5. The cooling and compression time per step varied from a maximum of 3 ms to a minimum of 100 μs with a total cooling and compression time of 115 ms. The cooling time at the beginning of the compression scheme is longer since the change in well area is larger. Near the end of the simulation, when the compression steps are fairly equal, the cooling time was ~ 1.2 ms per step. The final compression captured 77.7% of the atoms in the central well with 84.8% of the atoms within a 20 μm square around the central spot. The loss of atoms in the central well is due to the initial placement of the Gaussian cloud in the optical potential, the temperature of the atoms, and the discrete nature of the SLM. The largest loss of atoms occurs in the first stage of compression where the percent change in well area is about 160%. About 9% of the atoms are lost in the first step, see Fig. 6. This initial loss could be reduced at the expense of higher laser power by having more SLM pixels or deeper wells. Once the cloud is safely contained in the lattice site, there is a steady decrease in atoms since the effective well depth of the trap is 3 mK and the temperature of the cloud is kept around 175 μK, which leads to a nonzero escape rate. Even though the total number captured in the central well decreases, the density of the atoms, defined as the number of atoms within the central well divided by the volume of the well, still increases after every step as shown in Fig 6.

4. Discussion

The final density of the cloud will be limited by both photon rescattering and atomic collisions. Typical high density MOTs provide densities $\sim 10^{11}$ cm^{-3} while dark MOTs(19) and dark optical lattices(20) have been used to reach $\sim 10^{12}$ cm^{-3}. Densities of order 10^{12} cm^{-3} have also been obtained in a highly anisotropic elongated bright MOT(21). We therefore expect that the final density achievable by this compression scheme will be on the order of 10^{12} cm^{-3}. For the parameters used above Fig. 6 shows that such a density is reached at the final compression stage for a MOT which initially contains only a single atom. The compression scheme may therefore be suitable for loading single atoms into sites of an optical lattice with sub wavelength periodicity. In this context the compression scheme provides an effective zoom lens with a magnification ratio of about 100 which would be difficult to achieve with a conventional design. Additional numerical simulations show that it is possible to direct the atoms into a preferred lattice site, instead of the central site, by introducing a small phase shift between the beams at each compression step.

Although only a very small number of atoms will fit into a wavelength scale lattice site without exceeding density limits imposed by optical cooling the intermediate stage of the compression appears attractive for creating atomic ensembles with large optical depth. This is of interest for studying quantum state mapping between light and small atomic ensembles(22).

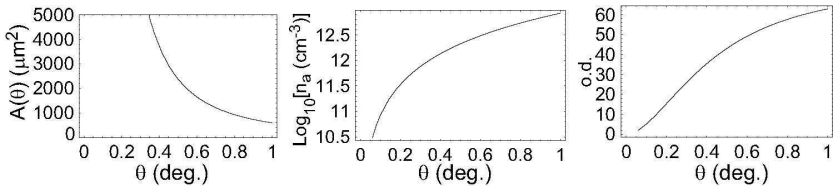

Fig. 7. Lattice well area (left), peak density (center) and optical depth (right) as a function of the beam angle θ. The calculations assumed $w_z = 0.1$ cm, a relative temperature of $k_B T_a/U_0 = 0.15/6. = .025$ and that 80% of the $N = 10^4$ atoms initially in the MOT are captured into the lattice site.

The initial, spherically symmetric MOT cloud has an optical depth, for a narrow beam with a width that is small compared to the MOT, of $od = \int_{-\infty}^{\infty} dz\, \sigma n_a(x=0, y=0, z)$ where $n_a(x,y,z)$ is the atomic density and $\sigma = 3\lambda_a^2/(2\pi)$ is the resonant cross section for a two-level atom with transition wavelength λ_a. Assuming for example a MOT with Gaussian density distribution with $\sigma_x = \sigma_y = \sigma_z = 50$ μm as in the previous section, and $N = 10^4$ atoms we find $od = 0.2$, which would imply a very weak interaction between a probe beam and the MOT atoms.

However, these same 10^4 atoms can be rapidly compressed into a cigar shaped lattice site to achieve an optical depth of about 35. To show this we examine the regime where the atomic temperature is small compared to the well depth (as in our numerical simulations). The atomic density distribution inside each elongated well will then be Gaussian with $\sigma_x = \sigma_y = [\Lambda(\theta)/(\sqrt{2}\pi)]\sqrt{k_B T_a/U_0}$, and $\sigma_z = (w_z/2)\sqrt{k_B T_a/U_0}$. The atomic density distribution can then be approximated by

$$n_a(x,y,z) = \frac{N}{(2\pi)^{3/2}\sigma_x\sigma_y\sigma_z} e^{-\left(x^2/2\sigma_x^2 + y^2/2\sigma_y^2 + z^2/2\sigma_z^2\right)} \tag{4}$$

We can define the optical depth as $od = -\ln(P_{\rm out}/P_{\rm in})$ where $P_{\rm in}, P_{\rm out}$ are the power incident on and after the atomic cloud. Accounting for the Gaussian transverse distribution of a radially symmetric laser beam and its' diffractive spreading as it propagates along the cloud we find

$$od = \frac{4\sigma}{w_0^2}\int_{-L/2}^{L/2} dz \int_0^{\infty} d\rho\, \rho n_a(\rho, z) \frac{1}{1 + z^2/z_R^2} e^{-2\rho^2/[w_0^2(1+z^2/z_R^2)]}, \tag{5}$$

where $\rho = \sqrt{x^2+y^2}$, w_0 is the beam waist and $z_R = \pi w_0^2/\lambda$. This expression is valid provided the beam intensity is everywhere small so that there is no saturation of the absorption. When the atomic density has a Gaussian profile as in Eq. (4) we can extend the limits of the z integration to $\pm\infty$ and get the analytical expression

$$od = N\frac{3\lambda}{\sqrt{2\pi}\sigma_z} \frac{e^{\frac{z_R^2(1+4\sigma_x^2/w_0^2)}{2\sigma_z^2}}}{\sqrt{1+4\sigma_x^2/w_0^2}} \mathrm{Erfc}\left[\frac{z_R\sqrt{1+4\sigma_x^2/w_0^2}}{\sqrt{2}\sigma_z}\right], \tag{6}$$

where $\mathrm{Erfc}(z) = 1 - (2/\sqrt{\pi})\int_0^z dt\, e^{-t^2}$ is the complementary error function.

Figure 7 shows the calculated well area, peak density, and optical depth as a function of beam angle θ for $N = 10^4$ atoms initially in the MOT. At $\theta = 0.4$ deg. the peak density reaches the photon rescattering limit of about 10^{12} cm^{-3}, but the optical depth along z is $od = 35$ for a probe beam with waist $w_0 = 3.0$ μm. This is a factor of 175 increase compared to the value in

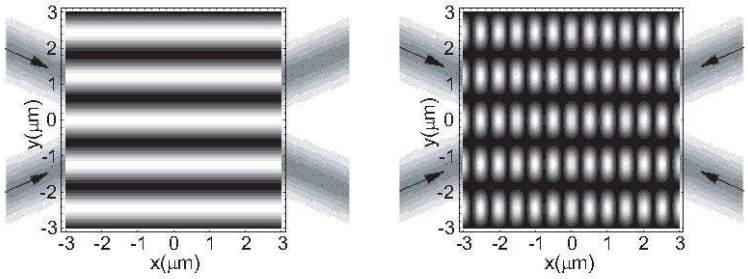

Fig. 8. Comparison of two interfering traveling waves (left) and two interfering standing waves (right) with high intensity shown in white. Both interference patterns are created with θ=π/8 givingπ/4 between beams. The traveling wave produces a 1D interference pattern while the standing wave produces a 2D lattice structure. The incident beam propagation directions are shown superimposed behind the plots.

the initial MOT, and is large enough to allow close to complete absorption of a photon in the atomic cloud. The radial optical depth is less than unity which implies that the cloud is optically thin for radially directed photons so heating due to photon rescattering will be minimized(21). This approach to compression is an alternative to anisotropic magnetic traps(23). Using the same beam parameters as in Sec. 3, but with $w_z = 0.1$ cm and only needing to illuminate 14 strips on the SLM, we would need about 1 W of power for each pair of beams.

Finally we consider some alternative compression geometries. The compression scheme with four traveling waves was chosen since it has a relatively simple experimental setup and compression in 2D can occur in one step. One drawback is that the wells are connected at 50% of the intensity. This effectively wastes half of the well depth requiring better cooling and more powerful lasers. There are alternative configurations that do not suffer from this problem. If all the laser beams initially propagate in the same direction, say $\theta = 0$, there will be no interference pattern. Each beam can then be moved in a particular direction to its final position. If the beams are moved smoothly, the optical potential also changes smoothly. For example, starting with three lasers beams propagating along $\theta = 0$ and smoothly moving two of the beams to $\theta = 120$ deg and $\theta = -120$ deg, the atoms will be compressed into the central well whose final area is a very small $A = 2\lambda^2/(3\sqrt{3}) = 0.38\lambda^2$. However, this requires a chamber with 240 deg. of access. If the final positions cannot be reached due to chamber limitations, the final cloud will be asymmetric.

Another approach relies on retro-reflecting the beams to create standing waves. Keeping the same configuration as the two traveling waves case, the result of interfering all four beams comprising the two standing waves is

$$I(x,y) \sim \cos^2(kx\cos(\theta))\cos^2(ky\sin(\theta)). \tag{7}$$

This results in a two-dimensional intensity pattern, as opposed to the traveling wave case which results in a one-dimensional lattice, see Fig. 8. The compression has to be done in steps, see Fig. 9. In the first step, a pair of beams with bisector along $\hat{x}$ is separated which compresses the atoms along the $\hat{y}$ axis, while they fill wells which are distributed along $\hat{x}$. Then the process is repeated for a pair of beams with bisector along $\hat{y}$. Increasing θ now results in compression along the $\hat{x}$ direction. Since after step 1, all of the atoms are located in wells along the x-axis,

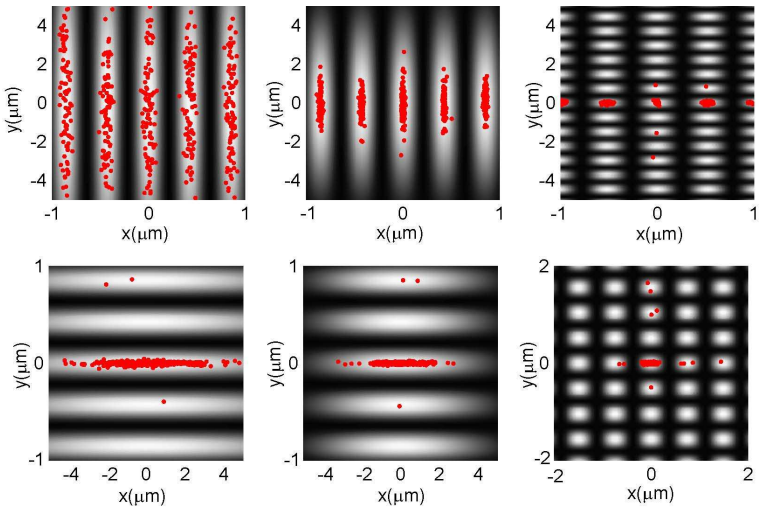

Fig. 9. (Color Online) Compression schematic using standing waves. The first step (top row) uses 2 pairs of standing waves with bisector along $\hat{x}$. The second step (bottom row) uses 2 pairs of standing waves with bisector along $\hat{y}$. This simulation uses the same beam parameters given in Section 3.

at the beginning of step 2, all of the atoms should be trapped in the central trough of the 1D standing wave on the x-axis. As in step 1, as θ increases, the area of the wells decrease and all the atoms will be compressed to a single well located at $x = y = 0$ with well area of $A = \lambda^2/2$. Contrasting with the traveling wave case, all of the wells are completely separated which is a more efficient usage of laser power. Experimentally, however, a retroreflection arrangement is more difficult to implement.

In conclusion the result of the protocol described here is two-dimensional compression of a cloud of atoms. While this paper focuses on two-dimensional compression, three-dimensional compression is also possible by adding two more traveling waves whose bisector is along $\hat{z}$. The result is a three-dimensional lattice which compresses in the same manner as the two-dimensional case.

The results of numerical simulations show that a high percentage of atoms can be compressed from an atomic cloud with a standard deviation of ~ 50 μm to a lattice site with area $A = 0.55$ μm^2. This is possible for a small number of atoms such that the final density does not exceed limits set by photon scattering and collisions. We also show that a partial compression up to beam angles of $\theta \sim 0.4$ deg. is an effective way of capturing atoms from a small, low optical density MOT, into a pencil shaped optical trap with $od = 35$. An atomic sample confined in this way is well suited for experiments requiring strong interactions between light and atomic ensembles.

This work was supported by an Advanced Opportunity Fellowship from the University of Wisconsin and NSF grant CCF-0523666 .